Journal of Biomolecular NMR **28:** 165–172, 2004.
KLUWER/ESCOM

An isotope labeling strategy for methyl TROSY spectroscopy

Vitali Tugarinov & Lewis E. Kay
Protein Engineering Network Centres of Excellence and the Departments of Medical Genetics, Biochemistry and Chemistry, University of Toronto, Toronto, Ontario, Canada M5S 1A8

Received 3 July 2003; Accepted 1 August 2003

Key words: deuteration, isotopic labeling, methyl protonation, methyl TROSY NMR

Abstract

Recently we have shown that HMQC spectra of protonated methyl groups in high molecular weight, highly deuterated proteins have large enhancements in sensitivity and resolution relative to HSQC-generated data sets. These enhancements derive from a TROSY effect in which complete cancellation of intra-methyl ^{1}H-^{1}H and ^{1}H-^{13}C dipolar interactions occurs for 50% of the signal in the case of HMQC, so long as the methyl is attached to a molecule tumbling in the macromolecular limit (Tugarinov, V., Hwang, P.M., Ollerenshaw, J.E., Kay, L.E. *J. Am. Chem. Soc.* (2003) **125**, 10420–10428; Ollerenshaw, J.E., Tugarinov, V. and Kay, L.E. *Magn. Reson. Chem.* (2003) **41**, 843–852. The first demonstration of this effect was made for isoleucine δ1 methyl groups in a highly deuterated 82 kDa protein, malate synthase G. As with ^{1}H-^{15}N TROSY spectroscopy high levels of deuteration are critical for maximizing the TROSY effect. Here we show that excellent quality methyl TROSY spectra can be recorded on U-[^{2}H] Ileδ1-[$^{13}CH_3$] Leu,Val-[$^{13}CH_3/^{12}CD_3$] protein samples, significantly extending the number of probes available for structural and dynamic studies of high molecular weight systems.

Introduction

The development of new NMR methodology for the study of high molecular weight systems continues to be a major focus of research efforts in many laboratories. In the past several years parallel advances in both labeling (Gardner and Kay, 1998; Goto and Kay, 2000) and pulse sequence technologies (Wider and Wüthrich, 1999) have significantly impacted on the range of problems that can be investigated using NMR approaches. At the forefront of these efforts has been the design of TROSY-based pulse schemes (Pervushin et al., 1997, 1998) which have facilitated the study of a number of proteins on the order of 100 kDa, including the homooctameric protein, 7,8-dihydroneopterin aldolase (Salzmann et al., 2000) and the 723-residue single polypeptide enzyme, malate synthase G (Tugarinov and Kay, 2003; Tugarinov et al., 2002). TROSY-experiments, to date, have concentrated on backbone ^{1}H-^{15}N spin systems and exploited cross-correlated relaxation between dipolar and chemical shift anisotropy interactions to optimize operative relaxation times and concomitantly spectral sensitivity and resolution. Very recently, we have shown that the TROSY effect is not limited to simple AX spin systems but can be extended to methyl spins in a $^{13}CH_3$ spin system as well (Ollerenshaw et al., 2003; Tugarinov et al., 2003). This has important consequences for studies of high molecular weight proteins because methyls (i) are excellent probes of both molecular structure and dynamics (Gardner et al., 1997; Metzler et al., 1996; Mueller et al., 2000; Nicholson et al., 1992; Skrynnikov et al., 2001), (ii) are most often localized to hydrophobic cores of proteins or molecular interfaces (Janin et al., 1988) so that methyl-methyl distances provide extremely valuable restraints in structural studies (Gardner et al., 1997; Metzler et al., 1996; Mueller et al., 2000) and (iii) often give rise to high intensity correlations in ^{1}H-^{13}C spectra that are reasonably well resolved (Gardner et al., 1997). In addition, the methyls of Ile (δ1 only), Leu and Val can be specifically protonated in an otherwise highly deuterated environment (Gardner and Kay, 1997; Goto et al., 1999), preserving the relax-

ation benefits of perdeuteration while maintaining a sufficient number of protons to probe important issues concerning molecular structure and dynamics.

In a previous set of papers (Tugarinov et al., 2003; Ollerenshaw et al., 2003) we have shown that the simple HMQC pulse scheme (Bax et al., 1983; Mueller, 1979) is, in fact, optimal 'as is' for ^{1}H-^{13}C methyl-TROSY correlation spectroscopy. Half of the originating magnetization in this experiment relaxes rapidly in both ^{1}H and ^{13}C time domains, while a second half relaxes with much smaller rates. Most importantly, in the absence of relaxation contributions from external protons, the pathways involving the slow and fast relaxing components *do not interchange*, so that the slowly relaxing component remains uncontaminated throughout the experiment. The slow relaxation of magnetization that traverses the TROSY pathway in the HMQC experiment is the result of extensive cancellation of intra-methyl ^{1}H-^{1}H and ^{1}H-^{13}C dipolar relaxation interactions that occurs for methyl groups attached to molecules tumbling in the macromolecular limit (Kay and Prestegard, 1987; Kay and Torchia, 1991; Muller et al., 1987; Werbelow and Marshall, 1973) and for this reason the TROSY effect in this case is magnetic field independent. The separation of TROSY- and anti-TROSY pathways mentioned above is in direct contrast to what occurs in the much more popular HSQC scheme (Bodenhausen and Rubin, 1980). Here the increased number of ^{1}H 90° pulses (relative to the HMQC sequence) leads to the interchange of fast and slowly relaxing components, impacting in a very negative way on both sensitivity and resolution in methyl ^{1}H-^{13}C spectra of high molecular weight proteins (Ollerenshaw et al., 2003; Tugarinov et al., 2003).

We first demonstrated this exclusively dipolar methyl TROSY effect on U-[^{2}H,^{15}N] Ile δ1-[$^{13}CH_3$] samples of (i) malate synthase G (MSG) at 37 °C (82 kDa, correlation time, τ_C, of 45 ns) and at 5 °C (τ_C = 118 ns) and of (ii) ClpP at 5 °C (305 kDa, $\tau_C \sim$ 400–450 ns) (Tugarinov et al., 2003). Average sensitivity gains of between 2 to 3 were obtained in a comparison of correlations in HMQC and HSQC spectra, in addition to improvements in resolution. Initial experiments focussed on samples that were protonated exclusively at the δ1 position of Ile in order to minimize methyl relaxation with external proton spins since such relaxation contributions can be quite detrimental to the methyl TROSY effect. Samples labeled only at the Ile positions are of somewhat limited utility, however, since only a single class of probe is available for structural and dynamical studies. It is, therefore, of considerable practical importance to establish how additional protonation at methyl sites might influence the quality of HMQC spectra. For example, can strong TROSY effects still be observed in much more useful methyl protonated Ile, Leu and Val samples? Here we show which indeed this is the case and present a methyl labeling scheme that optimizes this TROSY enhancement.

Materials and methods

Four U-[^{2}H,^{15}N] samples of MSG in D_2O with different patterns of methyl protonation have been prepared for analysis including: i) U-[^{2}H,^{15}N] Ileδ1-[$^{13}CH_3$] MSG that was used in our previous work (Tugarinov et al., 2003), ii) U-[^{2}H,^{15}N] Leu,Val-[$^{13}CH_3$/$^{13}CH_3$] MSG with both Leu and Val methyls of the $^{13}CH_3$ variety, iii) U-[^{2}H,^{15}N] Leu,Val-[$^{13}CH_3$/$^{12}CD_3$] with one Leu(Val) methyl group $^{13}CH_3$ and the second $^{12}CD_3$ and iv) U-[^{2}H,^{15}N] Ileδ1-[$^{13}CH_3$] Leu,Val-[$^{13}CH_3$/$^{12}CD_3$] - the same as sample iii but with Ile δ1 methyls of the $^{13}CH_3$ variety. All samples were prepared as described in detail elsewhere (Tugarinov et al., 2002, 2003; Tugarinov and Kay, 2003) using D_2O-based media and [^{12}C,^{2}H]-D-glucose as the main carbon source. For selective protonation of methyl groups the appropriate combinations of biosynthetic precursors were used including 2-keto-3,3-d_2-4-^{13}C-butyrate for Ile δ1 $^{13}CH_3$ labeling, 2-keto-3-methyl-^{13}C-3-d_1-4-^{13}C-butyrate for $^{13}CH_3$ labeling of both Val and Leu methyls ($^{13}CH_3$/$^{13}CH_3$), and 2-keto-3-methyl-d_3-3-d_1-4-^{13}C-butyrate for the non-stereospecific labeling of the two Leu/Val methyls as $^{13}CH_3$/$^{12}CD_3$. All compounds are commercially available from Isotec (although the latter is a custom synthesis) with deuteration at position 3 achieved by exchange in D_2O as described previously (Gardner and Kay, 1997; Goto et al., 1999). Alternatively, the precursors can be prepared using inexpensive synthetic procedures analogous to those described earlier (Gross et al., 2003; Hajduk et al., 2000). Although ^{15}N labeling is not essential for the experiments described here, we have labeled all our proteins with ^{15}N in the event that ^{1}H-^{15}N correlation experiments are desired. Protein concentrations were 0.61 mM, 0.71 mM, 0.71 mM and 0.63 mM for U-[^{2}H,^{15}N] Ileδ1-[$^{13}CH_3$], U-[^{2}H,^{15}N] Leu,Val-[$^{13}CH_3$/$^{13}CH_3$], U-[^{2}H,^{15}N] Leu,Val-[$^{13}CH_3$/$^{12}CD_3$] and U-[^{2}H,^{15}N] Ileδ1-[$^{13}CH_3$] Leu,Val-[$^{13}CH_3$/$^{12}CD_3$] MSG samples,

respectively, in 99% D_2O, 25 mM sodium phosphate, pH 7.1 (uncorrected), 20 mM $MgCl_2$, 0.05% NaN_3, 0.1 mg mL^{-1} Pefabloc and 5 mM DTT.

HMQC and HSQC spectra at 37 °C were acquired using pulse schemes described previously (Tugarinov et al., 2003) with $t_{1,max}(t_{2,max})$ values of 105 ms (64 ms), 4 scans/FID and a repetition delay of 1.5 s. Spectra at 5 °C were obtained with $t_{1,max}$ = 45 ms, $t_{2,max}$ = 64 ms and 32 scans/FID with a repetition delay of 1.5 s. Spectral widths in the $^{13}C(t_1)$ dimension were 9 ppm, 12 ppm, 12 ppm and 21 ppm for U-[^{2}H,^{15}N] Ileδ1-[$^{13}CH_3$], U-[^{2}H,^{15}N] Leu,Val-[$^{13}CH_3$/$^{13}CH_3$], U-[^{2}H,^{15}N] Leu,Val-[$^{13}CH_3$/$^{12}CD_3$] and U-[^{2}H,^{15}N] Ileδ1-[$^{13}CH_3$] Leu,Val-[$^{13}CH_3$/$^{12}CD_3$] MSG samples, respectively. All the spectra were processed identically with NMRPipe/NMRDraw software (Delaglio et al., 1995) using 36° and 54°-shifted sine-bell squared window functions in t_1 and t_2, respectively. Unless indicated otherwise all spectra were recorded at a field strength of 800 MHz (^{1}H frequency).

Results and discussion

Figure 1a shows a conventional ^{1}H-^{13}C HSQC spectrum recorded on a U-[^{2}H,^{15}N] Leu,Val-[$^{13}CH_3$/$^{13}CH_3$] sample of MSG. By means of comparison a ^{1}H-^{13}C HMQC correlation map of U-[^{2}H,^{15}N] Leu,Val-[$^{13}CH_3$/$^{12}CD_3$] MSG is presented in Figure 1b. Although both samples are of equal protein concentration (0.71 ± 0.05 mM) it is clear that significant gains in resolution are accompanied by substantially higher signal-to-noise (S/N) ratios in the HMQC spectrum of the U-[^{2}H,^{15}N] Leu,Val-[$^{13}CH_3$/$^{12}CD_3$] sample. S/N gains for correlations in the spectrum of Figure 1b relative to the corresponding peaks of Figure 1a are quantified in the histogram of Figure 1c (37 °C, τ_C = 45 ns), with an average increase of a factor of 1.7. At 5 °C (τ_C = 118 ns) the relative S/N gain is 3.5 (Figure 1d). Thus, the loss of a factor of two in concentration of NMR-active methyls in the case of $^{13}CH_3$/$^{12}CD_3$ Leu/Val methyl labeling is (very significantly) more than compensated for by the improved relaxation properties of the remaining $^{13}CH_3$ groups.

We have chosen the HSQC correlation spectrum recorded on a U-[^{2}H,^{15}N] Leu,Val-[$^{13}CH_3$/$^{13}CH_3$] MSG sample as the 'reference' in Figure 1 since the labeling scheme employed (i.e., methyls of Leu and Val are both of the $^{13}CH_3$ variety) and the pulse sequence used are 'conventional' in the sense that they are routinely used by many laboratories. The HMQC data set of the U-[^{2}H,^{15}N] Leu,Val-[$^{13}CH_3$/$^{12}CD_3$] MSG sample, Figure 1b, is superior in terms of both sensitivity *and* resolution relative to data sets recorded with other labeling/pulse scheme combinations. This is illustrated in Figure 2 where a small section of the correlation maps in Figure 1 (marked by the dashed rectangles) is plotted for many of the combinations of labeling strategies and experiments that are possible, along with averaged, normalized S/N values, $\langle S/N \rangle_N$. Finally, we note that HMQC spectra recorded on U-[^{2}H,^{15}N] Ile δ1-[$^{13}CH_3$] Leu,Val-[$^{13}CH_3$/$^{12}CD_3$] MSG samples are of essentially identical quality to those recorded on samples with protonation restricted to Leu and Val. Thus, the addition of protons to Ile δ1 methyl groups does not deteriorate the methyl TROSY effect for Leu and Val.

In order to gain insight into the sensitivity and resolution improvements discussed above we have measured free-precession T_2 relaxation times of (i) ^{1}H-^{13}C double quantum/zero quantum (DQ/ZQ) coherences (average of DQ and ZQ T_2 values), (ii) single quantum (SQ) ^{13}C and (iii) SQ ^{1}H coherences of methyl groups in MSG (37 °C). These are the relevant relaxation times for a description of the HMQC and HSQC pulse schemes compared above. Recall that in the case of the HMQC (HSQC) the flow of coherence is, $I_{tr} \rightarrow I_{tr}C_{tr} \rightarrow I_{tr}$, ($I_{tr} \rightarrow C_{tr} \rightarrow I_{tr}$), where I and C are methyl ^{1}H and ^{13}C operators and the subscript '*tr*' indicates transverse terms. As described in detail elsewhere, in the macromolecular limit the decay of each of the above coherences can be described to very good approximation by two time constants (fast and slow) (Ollerenshaw et al., 2003; Tugarinov et al., 2003). The slow time constants are of interest here since for very large proteins only the slowly relaxing components contribute to the final signal. The T_2 values of the slowly relaxing ^{1}H-^{13}C DQ/ZQ and ^{1}H coherences are readily obtained by pulse schemes which are slightly modified versions of the standard HMQC sequence (Tugarinov et al., 2003). The decay of the slowly relaxing ^{13}C SQ elements can be measured using an HSQC scheme whereby magnetization originates on ^{13}C and where the fast relaxing components are again not observed in spectra. A detailed description of the experiments is beyond the scope of the presentation here (pulse sequence code is available from the authors upon request).

Typical relaxation decay curves for the coherences listed above from Ile, Leu and Val methyls in MSG samples with different methyl labeling schemes are

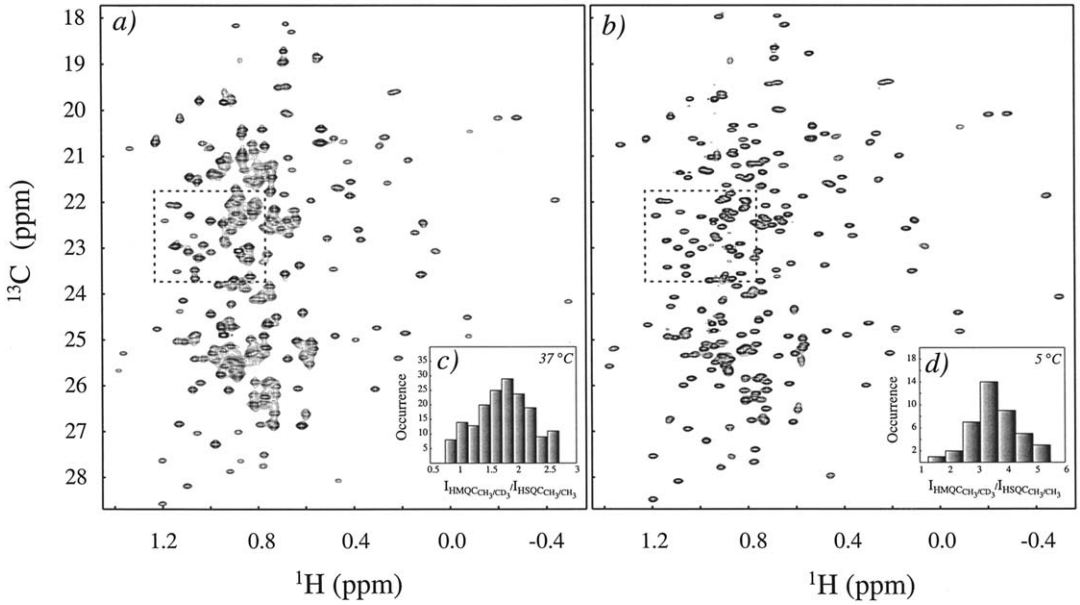

Figure 1. Comparison of the ^{1}H-^{13}C HSQC spectrum of U-[^{2}H,^{15}N] Leu,Val-[$^{13}CH_3/^{13}CH_3$] MSG (a) with the HMQC spectrum of U-[^{2}H,^{15}N] Leu,Val-[$^{13}CH_3/^{12}CD_3$] MSG (b) recorded at 37 °C, 800 MHz. Both spectra were acquired with identical acquisition times (see Materials and Methods), processed identically and are plotted with the same contour levels. The spectral regions enclosed in dashed rectangles in (a) and (b) are enlarged in Figure 2. Histograms of ratios of peak signal-to-noise values in the HMQC data set versus the HSQC map at 37 °C (c) and 5 °C (d) were obtained for a subset of well separated peaks in both spectra.

Table 1. Average free-precession T_2 relaxation times of ^{1}H-^{13}C DQ/ZQ, ^{13}C SQ and ^{1}H SQ coherences and ^{1}H T_1 relaxation times of Ile, Leu and Val methyls in malate synthase G, D_2O at 37 °C measured on samples prepared with different Ile, Leu, Val-labeling methods[a]

Type of residue compared	Labeling type	^{1}H-^{13}C DQ/ZQ T_2(ms)	^{13}C SQ T_2 (ms)	^{1}H SQ T_2 (ms)	^{1}H T_1 (s)	$\langle\zeta\rangle$[b] (Å)
Ile	Ileδ1 - [$^{13}CH_3$]	57.6 ± 19.6[c]	49.4 ± 12.8[c]	44.2 ± 14.1[c]	1.6 ± 0.4	5.5
	Ileδ1 - $^{13}CH_3$, Leu, Val-[$^{13}CH_3/^{12}CD_3$]	44.1 ± 16.1	40.3 ± 11.4	35.4 ± 9.7	1.2 ± 0.3	3.5
Leu, Val	Leu,Val-[$^{13}CH_3/^{12}CD_3$]	37.9 ± 10.3	31.4 ± 8.0	32.0 ± 8.7	0.60 ± 0.1	3.9
	Leu, Val-[$^{13}CH_3/^{13}CH_3$]	20.0 ± 3.5	25.9 ± 5.1	22.1 ± 5.3	0.62 ± 0.2	2.4
	Ileδ1 - $^{13}CH_3$, Leu, Val-[$^{13}CH_3/^{12}CD_3$]	38.8 ± 11.5	33.7 ± 9.2	33.8 ± 11.0	0.64 ± 0.2	3.5

[a]All relaxation times were measured at 800 MHz unless indicated otherwise; the pulse-sequences used to extract the relaxation times are available from the authors. The relaxation times were quantified and averaged for 25 (Ile) and 87 (Leu + Val) completely resolved, unambiguously assigned peaks whose relaxation decays (all coherence types) could be well fit to a mono-exponential function of the form A $\exp(-t/T_2)$, where t is the parametrically varied relaxation delay (± values indicate 1 standard deviation from the average, based on measured values for Ile and Leu+Val).

[b]$\langle\zeta\rangle = \langle(\sum_i 1/r_{HH_i}^6)^{-1/6}\rangle$ is the average effective sum of distances between methyl protons of a given residue type and external protons H_i (external protons refer to all protons resulting from the particular labeling scheme employed that are not part of the methyl group in question) where the angular brackets denote averaging over all residues of a given type. For example, ζ, is computed from the x-ray structure of MSG (Howard et al., 2000) for each Ile and subsequently all ζ values averaged to get $\langle\zeta\rangle$ for Ile.

[c]Measured at 600 MHz.

shown in Figure 3, while Table 1 summarizes the average relaxation times obtained. Also included in the Table are the average effective sum of distances between methyl protons of a given residue type (for

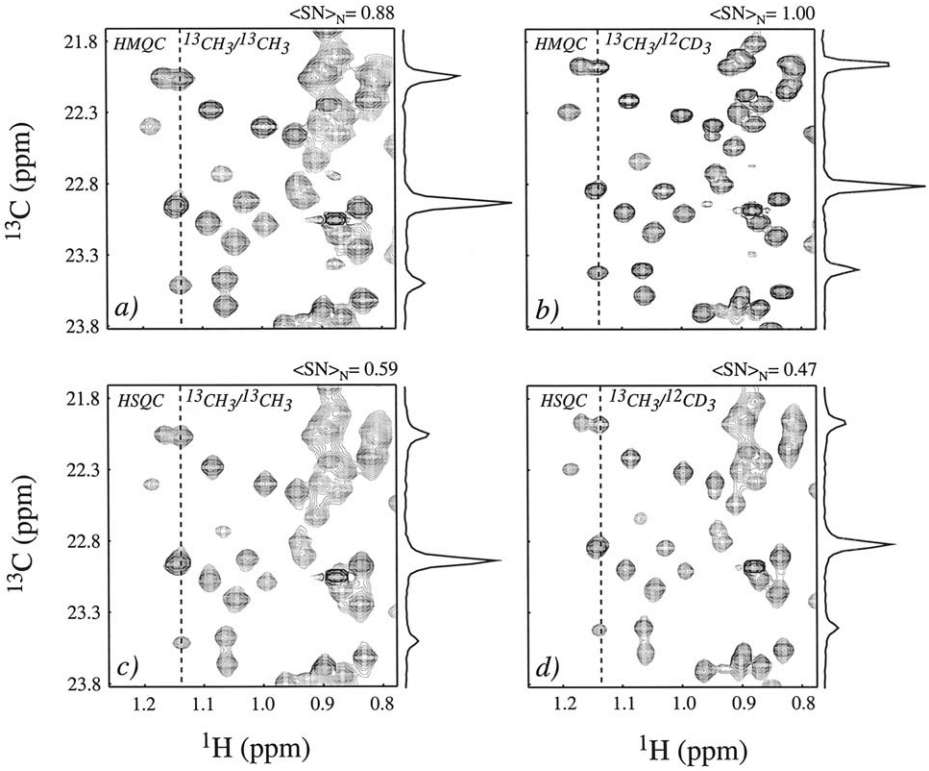

Figure 2. Comparison of S/N and resolution in HMQC and HSQC spectra of MSG, 37 °C, 800 MHz, labeled as indicated. Samples compared were 0.7 mM U-[^{2}H,^{15}N] Leu,Val-[^{13}CH$_3$/^{13}CH$_3$] MSG (referred to as ^{13}CH$_3$/^{13}CH$_3$) and 0.7 mM U-[^{2}H,^{15}N] Leu,Val-[^{13}CH$_3$/^{12}CD$_3$] MSG (referred to as ^{13}CH$_3$/^{12}CD$_3$). All spectra are recorded and processed identically and are shown with the same contour levels, with one-dimensional traces along the ^{13}C dimension at the chemical shift indicated by dashed lines shown beside each spectrum. Visible differences in ^{13}C chemical shifts between the spectra (see for example, (a) and (b)) arise from a three-bond isotope shift due to deuteration/protonation of the second methyl group in Leu and Val. This average isotope shift ($^3\Delta_{[CD3\Rightarrow CH3]}$) is 85±15 ppb for 154 peaks that are well separated in all spectra. The average normalized signal-to-noise, $\langle S/N\rangle_N$, indicated at the top of each spectrum corresponds to an average obtained over 154 well resolved peaks (same peaks quantified in each spectrum). The $\langle S/N\rangle_N$ for a spectrum is calculated by taking the ratio of (i) the S/N value for peak *j* in that spectrum and (ii) the S/N of the corresponding peak in the HMQC spectrum recorded on the U-[^{2}H,^{15}N] Leu,Val-[^{13}CH$_3$/^{12}CD$_3$] MSG sample and averaging over all such peaks *j*. Expressions for the functional forms of the signal intensity in HSQC and HMQC correlation maps are given in Equations 3 and 5 of Tugarinov et al. (2003) and provide insight into the origins of the sensitivity improvement associated with the HMQC scheme.

example Ile, Leu or Val) and external protons H_i, $\langle\zeta\rangle = \langle(\sum_i 1/r_{HH_i}^6)^{-1/6}\rangle$, obtained from the x-ray structure of the glyoxylate-bound form of the protein (Howard et al., 2000). The angular brackets denote averaging over all such distances, ζ, obtained from the different residues of a given type (*i.e*, average over all Ile, for example). In Figures 3a–c decays from Ile 147 in U-[^{2}H,^{15}N] Ileδ1-[^{13}CH$_3$] (red, ζ = 6.2 Å) and U-[^{2}H,^{15}N], Ileδ1-[^{13}CH$_3$,], Leu,Val-[^{13}CH$_3$/^{12}CD$_3$] (blue, ζ = 2.7 Å) samples of MSG are compared. The similar increases in decay rates of both ^{1}H-^{13}C DQ/ZQ ($I_{tr}C_{tr}$) and ^{1}H (I_{tr}) SQ coherences due to protonation at Leu/Val methyl side chains are expected since the relaxation properties of $I_{tr}C_{tr}$ and I_{tr} are affected in the same way by external protons (Tugarinov et al., 2003). The free-precession ^{13}C SQ (C_{tr}) decay is less influenced by external spins. The increase in relaxation rate in this case arises due to the inter-conversion between C_{tr}, $2C_{tr}I_{zi}$, $4C_{tr}I_{zi}I_{zj}$, $8C_{tr}I_{zi}I_{zj}I_{zk}$ from ^{1}H-^{13}C scalar coupled evolution (*i*,*j*,*k* are the three methyl protons) and concomitant proton spin flips which affect the anti-phase ^{13}C terms.

Figures 3d–f show the corresponding decay curves for one of the methyls of Leu 498 (δ^{13}C = 23.3 ppm, δ^1H = 0.62 ppm) measured from U-[^{2}H,^{15}N] Leu,Val-[^{13}CH$_3$/^{12}CD$_3$] (red, ζ = 2.5 Å), U-[^{2}H,^{15}N] Ileδ1-[^{13}CH$_3$,] Leu,Val-[^{13}CH$_3$/^{12}CD$_3$] (blue, ζ = 2.5 Å) and U-[^{2}H,^{15}N] Leu,Val-[^{13}CH$_3$/^{13}CH$_3$] (green, ζ = 1.9 Å) MSG samples. It is noteworthy that the decay rates of the coherences measured for Leu 498 in the

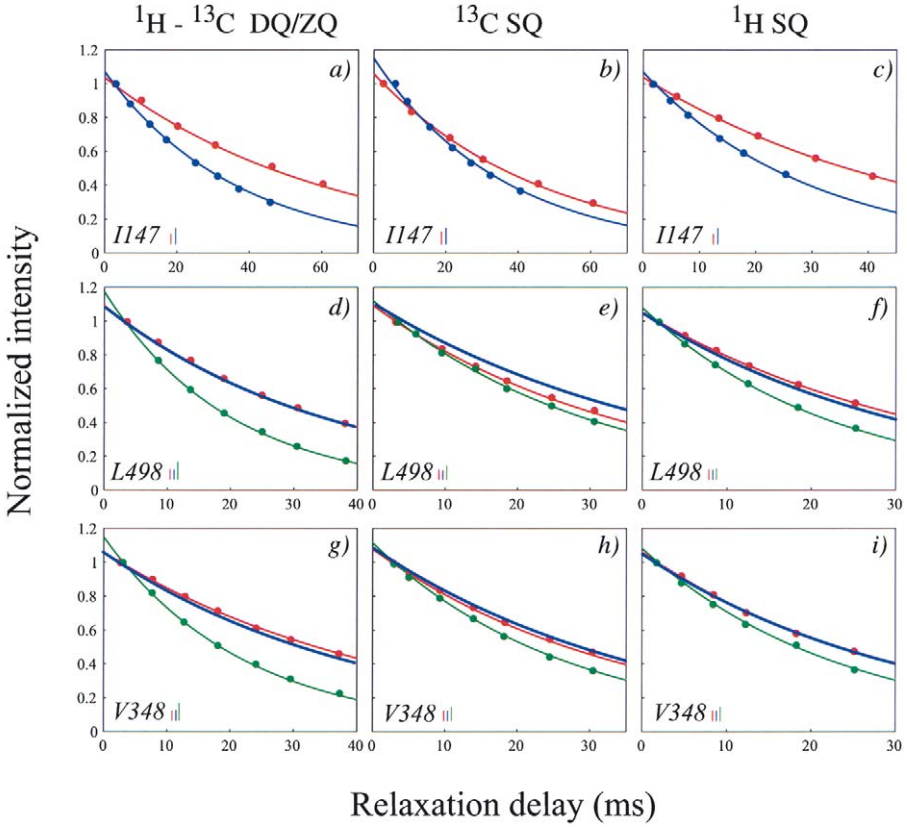

Figure 3. Typical relaxation decay curves (experimental data indicated with circles) best-fit with a single exponential decay function (fits in solid lines) for MSG samples prepared with different methyl labeling schemes. Data for the decay of ^{1}H-^{13}C DQ/ZQ, ^{13}C SQ and ^{1}H SQ coherences for Ile 147 (a–c), Leu 498 (d–f) and Val 348 (g–i) are indicated. Experimental data points and best fit decay curves for residues in U-[^{2}H,^{15}N] Ileδ1-[$^{13}CH_3$] MSG (a-c) and U-[^{2}H,^{15}N] Leu,Val-[$^{13}CH_3/^{12}CD_3$] MSG (d–i) are shown with red lines, while data from U-[^{2}H,^{15}N] Leu,Val-[$^{13}CH_3/^{13}CH_3$] MSG (d–i) and from U-[^{2}H,^{15}N] Ileδ1-[$^{13}CH_3$] Leu,Val-[$^{13}CH_3/^{12}CD_3$] MSG (a–i) are shown in green and blue, respectively. Experimental data points are not shown for data recorded on the U-[^{2}H,^{15}N] Ileδ1-[$^{13}CH_3$] Leu,Val-[$^{13}CH_3/^{12}CD_3$] sample (d–i) since for the most part they would fall on top of the red points (U-[^{2}H,^{15}N] Leu,Val-[$^{13}CH_3/^{12}CD_3$] MSG). All the measurements were made at 800 MHz ^{1}H frequency except for data recorded on the U-[^{2}H,^{15}N] Ileδ1-[$^{13}CH_3$] sample (red in a–c) which was obtained at 600 MHz. Errors in peak intensities were estimated from noise in the spectra and are showed with vertical bars at the bottom of each subplot.

Ile, Leu, Val protonated sample ($^{13}CH_3/^{12}CD_3$) are essentially the same as the corresponding rates obtained from the sample with protonation confined to Leu, Val methyl groups ($^{13}CH_3/^{12}CD_3$). Similar decay rates ('red' vs. 'blue' curves) are also observed for other residues as well (see Val 348 in Figures 3g–i) and explain why the sensitivity and resolution in the Leu/Val regions of spectra are not degraded by introduction of protons at the Ile δ1 position. In contrast, there is a slight decrease in sensitivity in the Ile region accompanying the introduction of protons at one of two methyl positions on each Leu/Val residue, by 20% on average. Protonation of a second methyl position in Leu and Val increases significantly the methyl relaxation rates, leading to substantial losses in both sensitivity and resolution (compare Figures 1a and b). The proposed Leu,Val-[$^{13}CH_3/^{12}CD_3$] labeling scheme is therefore critical for the optimization of the methyl TROSY effect.

The relative S/N of correlation maps recorded on samples prepared using the various methyl labeling schemes described above is also a function of the recovery of methyl ^{1}H magnetization to its equilibrium state. Although methyl ^{1}H longitudinal relaxation is expected to be multi-exponential due to cross-relaxation with other protons in the sample and cross-correlated relaxation involving intra-methyl spins, we have, nevertheless, obtained reasonable fits of ^{1}H magnetization recovery profiles to a single exponential model, and the ^{1}H T_1 values obtained in this manner are listed in Table 1 (800 MHz). Differences in average methyl ^{1}H T_1 values for Leu and Val residues ob-

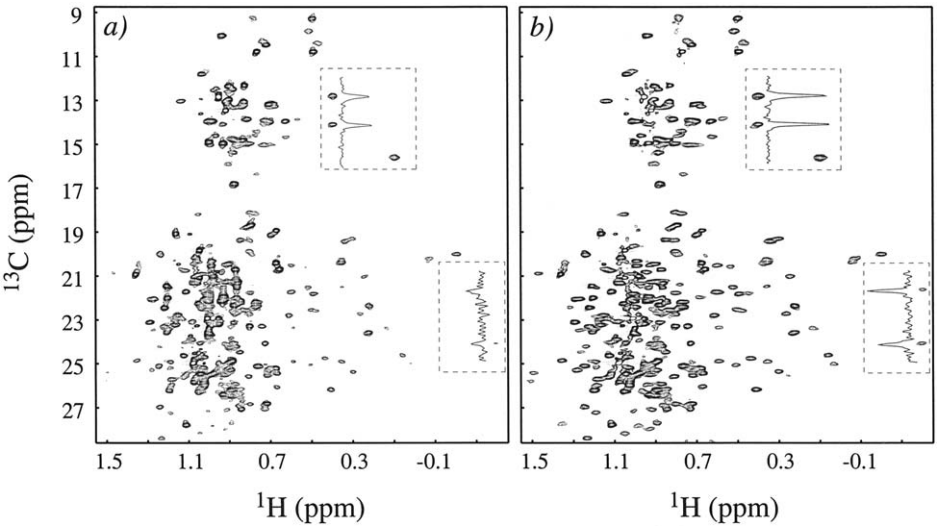

Figure 4. Comparison of HSQC (a) and HMQC (b) spectra recorded on a U-[^{2}H,^{15}N] Ileδ1-[$^{13}CH_3$] Leu,Val-[$^{13}CH_3/^{12}CD_3$] sample of MSG at 5 °C, 800 MHz (net acquisition time 2.5 h/spectrum).

tained in U-[^{2}H,^{15}N] Leu,Val-[$^{13}CH_3/^{13}CH_3$] and U-[^{2}H,^{15}N] Leu,Val-[$^{13}CH_3/^{12}CD_3$] MSG samples were very minor, while a 30% increase in Ile δ1 ^{1}H T_1 values was observed in a comparison of U-[^{2}H,^{15}N] Ileδ1-[$^{13}CH_3$] and U-[^{2}H,^{15}N] Ileδ1-[$^{13}CH_3$] Leu,Val-[$^{13}CH_3/^{12}CD_3$] MSG samples, Table 1. The addition of trace amounts of paramagnetic doping agents can expedite the recovery of ^{1}H magnetization to equilibrium, with minimal effects on line widths (Pintacuda and Otting, 2002), discussed recently in the context of ^{13}C spectroscopy of large proteins (Eletsky et al., 2003). However, since our goal is to use our samples for recording methyl-methyl NOE correlations, which would be seriously undermined with the addition of a paramagnetic agent, we have not done so here.

As a final demonstration of the inherent sensitivity of methyl correlation spectroscopy and the significant gains that can be obtained with HMQC relative to HSQC, we show in Figure 4 a comparison of HSQC (a) and HMQC (b) correlation maps recorded on a U-[^{2}H,^{15}N] Ileδ1-[$^{13}CH_3$] Leu,Val-[$^{13}CH_3/^{12}CD_3$] MSG sample at 5 °C (τ_c = 118 ns). An average gain of 2.6 in S/N is noted for the HMQC data set relative to its HSQC counterpart.

In summary, we have described an optimal isotope labeling strategy for methyl TROSY spectroscopy of large proteins involving replacement of one of the two methyl groups in each of Leu and Val with $^{12}CD_3$. The results presented here suggest that the production of U-[^{2}H] Ileδ1-[$^{13}CH_3$] Leu,Val-[$^{13}CH_3/^{12}CD_3$] protein samples in concert with HMQC methyl TROSY spectroscopy will facilitate the study of high molecular weight proteins and supramolecular complexes.

Acknowledgements

This work was supported by a grant from the Canadian Institutes of Health Research (CIHR) to L.E.K. We thank Dr C.T. Tan (Isotec, OH) for the synthesis of biosynthetic precursors used in this work. V.T. is a recipient of a Human Frontiers Science Program Postdoctoral Fellowship. L.E.K. holds a Canada Research Chair in Biochemistry.

References

Bax, A., Griffey, R.H. and Hawkings, B.L. (1983) *J. Magn. Reson.*, **55**, 301–315.

Bodenhausen, G. and Rubin, D.J. (1980) *Chem. Phys. Lett.*, **69**, 185–189.

Delaglio, F., Grzesiek, S., Vuister, G.W., Zhu, G., Pfeifer, J. and Bax, A. (1995) *J. Biomol. NMR*, **6**, 277–293.

Eletsky, A., Moreira, O., Kovacs, H. and Pervushin, K. (2003) *J. Biomol. NMR*, **26**, 167–179.

Gardner, K.H. and Kay, L.E. (1997) *J. Am. Chem. Soc.*, **119**, 7599–7600.

Gardner, K.H. and Kay, L.E. (1998) *Annu. Rev. Biophys. Biomol. Struct.*, **27**, 357–406.

Gardner, K.H., Rosen, M.K. and Kay, L.E. (1997) *Biochemistry*, **36**, 1389–1401.

Goto, N.K. and Kay, L.E. (2000) *Curr. Opin. Struct. Biol.*, **10**, 585–592.

Goto, N.K., Gardner, K.H., Mueller, G.A., Willis, R.C. and Kay, L.E. (1999) *J. Biomol. NMR*, **13**, 369–374.

Gross, J.D., Gelev, V.M. and Wagner, G. (2003) *J. Biomol. NMR*, 235–242.

Hajduk, P.J., Augeri, D.J., Mack, J., Mendoza, R., Yang, J.G., Betz, S.F. and Fesik, S.W. (2000) *J. Am. Chem. Soc.*, **122**, 7898–7904.

Howard, B.R., Endrizzi, J.A. and Remington, S.J. (2000) *Biochemistry*, **39**, 3156–3168.

Janin, J., Miller, S. and Chothia, C. (1988) *J. Mol. Biol.*, **204**, 155–164.

Kay, L.E. and Prestegard, J.H. (1987) *J. Am. Chem. Soc.*, 3829–3835.

Kay, L.E. and Torchia, D.A. (1991) *J. Magn. Reson.*, **95**, 536–547.

Metzler, W.J., Wittekind, M., Goldfarb, V., Mueller, L. and Farmer, B.T. (1996) *J. Am. Chem. Soc.*, **118**, 6800–6801.

Mueller, G.A., Choy, W.Y., Yang, D., Forman-Kay, J.D., Venters, R.A. and Kay, L.E. (2000) *J. Mol. Biol.*, **300**, 197–212.

Mueller, L. (1979) *J. Am. Chem. Soc.*, **101**, 4481–4484.

Mueller, N., Bodenhausen, G. and Ernst, R.R. (1987) *J. Magn. Reson.*, **75**, 297–334.

Nicholson, L.K., Kay, L.E., Baldisseri, D.M., Arango, J., Young, P.E., Bax, A. and Torchia, D.A. (1992) *Biochemistry*, **31**, 5253–5263.

Ollerenshaw, J.E., Tugarinov, V. and Kay, L.E. (2003) *J. Magn. Reson. Chem.*, **41**, 843–852.

Pervushin, K., Riek, R., Wider, G. and Wüthrich, K. (1997) *Proc. Natl. Acad. Sci. USA*, **94**, 12366–12371.

Pervushin, K., Riek, R., Wider, G. and Wüthrich, K. (1998) *J. Am. Chem. Soc.*, **120**, 6394–6400.

Pintacuda, G. and Otting, G. (2002) *J. Am. Chem. Soc.*, **124**, 372–373.

Salzmann, M., Pervushin, K., Wider, G., Senn, H. and Wüthrich, K. (2000) *J. Am. Chem. Soc.*, **122**, 7543–7548.

Skrynnikov, N.R., Mulder, F.A.A., Hon, B., Dahlquist, F.W. and Kay, L.E. (2001) *J. Am. Chem. Soc.*, **123**, 4556–4566.

Tugarinov, V. and Kay, L.E. (2003) *J. Mol. Biol.*, **327**, 1121–1133.

Tugarinov, V., Hwang, P.M., Ollerenshaw, J.E. and Kay, L.E. (2003) *J. Am. Chem. Soc.*, **125**, 10420–10428.

Tugarinov, V., Muhandiram, R., Ayed, A. and Kay, L.E. (2002) *J. Am. Chem. Soc.*, **124**, 10025–10035.

Werbelow, L.G. and Marshall, A.G. (1973) *J. Magn. Reson.*, 299–313.

Wider, G. and Wüthrich, K. (1999) *Curr. Opin. Struct. Biol.*, **9**, 594–601.